Malaysian Journal of Chemistry, 2025, Vol. 27(3), 314-331
(Special Issue: *International Conference on Sustainable Materials and Technologies, ICSMT 2025*)

Bio-derived Copper Oxide Nanostructure as Catalyst for 4-nitrophenol Reduction and Photo-degradation of Organic Pollutants

Devadason Princess Jeba[1]*, Shanmugasundaram Gurusamy[1] and Veerasamy Sathish[2]
[1]Department of Chemistry, V. O. Chidambaram College, Tuticorin, Tamil Nadu 628 008, India
Affiliated to Manonmaniam Sundaranar University, Abishekapatti, Tirunelveli-627012, Tamil Nadu, India
[2]Department of Chemistry, Bannari Amman Institute of Technology, Sathyamangalam-638 401, India
*Corresponding author (e-mail: dprincessjeba@gmail.com)

A sustainable and green synthesis of Copper Oxide nanoparticles (CuO NPs) are developed using aqueous leaf extract of Syzygium cumini. The optical, structural and morphological properties of the nanoparticles were analyzed using various spectral and microscopic techniques. Photocatalytic degradation of organic dyes utilizing CuO NPs as photo-catalyst has been investigated under visible light irradiation in aqueous solutions. The CuO nanoparticles exhibit excellent photocatalytic degradation of methylene blue, achieving a 98% degradation after 60 minutes under artificial light irradiation. These CuO nanoparticles demonstrate efficient photocatalytic activity, making them highly beneficial for water purification and other environmentally sustainable applications. CuO NPs serve as highly effective heterogeneous catalysts for the degradation of methylene blue dye. The change in λmax values and the evolution of oxygen gas indicated that the dye could be efficiently degraded by the photocatalyst without producing any hazardous waste. Additionally, the catalytic performance of the nanoparticles was assessed through the reduction of 4-nitrophenol. The catalyst demonstrates exceptional catalytic performance by efficiently converting 4-nitrophenol to 4-aminophenol in just 5 minutes, highlighting its remarkable effectiveness.

Keywords: CuO nanoparticles; Syzygium cumini; 4-nitrophenol; photodegradation; methylene blue

Received: January 2025; Accepted: April 2025

Green synthesis of nanostructured metals and metal oxides based on biological resources is an emerging technology that is economically viable and reduces the toxicity of nanoparticles commonly associated with conventional chemical synthesis. Among all the metal oxides, copper oxide nanoparticles (CuO NPs) due to their distinctive catalytic, electric, mechanical and thermal properties have gained significant importance and applications in industrial, environmental and medical fields [1–2]. CuO NPs in various shapes and morphologies like nanorods, nanowires, nanotubes, nanoflowers, nanoneedles and nanospheres were prepared through many synthetic routes such as electrochemical, sonochemical, microwave-assisted, oxidation–reduction, thermal, pyrolysis and precipitation [3-4]. These methods employ harsh reaction conditions, contribute to environmental pollution, and incur high costs. Therefore, in recent years, there has been a focus on developing non-hazardous, environmentally friendly, and cost-effective approaches to produce CuO NPs, aiming to minimize toxic substances in the environment [5]. Recently, there are many reports on the biosynthesis of CuO NPs using plant resources [6] and their applications in diverse fields viz. as catalyst for the degradation of dyes [7-9], C-S cross-coupling reaction [10-11], 1,3-cyclo-addition reaction [12] as anticancer and antibacterial agent [13], cytotoxic [14], plant defense booster [15].

Dyes are hazardous to environment and chemically stable with complex aromatic structure when discharged into the water bodies create alarming concern [16-18]. Various methods have been developed for treating industrial effluents [19, 20], but many simply transfer pollutants between phases or generate harmful byproducts, such as carcinogenic aromatic amines. Moreover, conventional techniques often demand large quantities of photocatalysts and produce significant amounts of sludge, posing additional environmental and health concerns. [21-22].

†Paper presented at the International Conference on Sustainable Materials and Technologies (ICSMT 2025)

Graphical Abstract

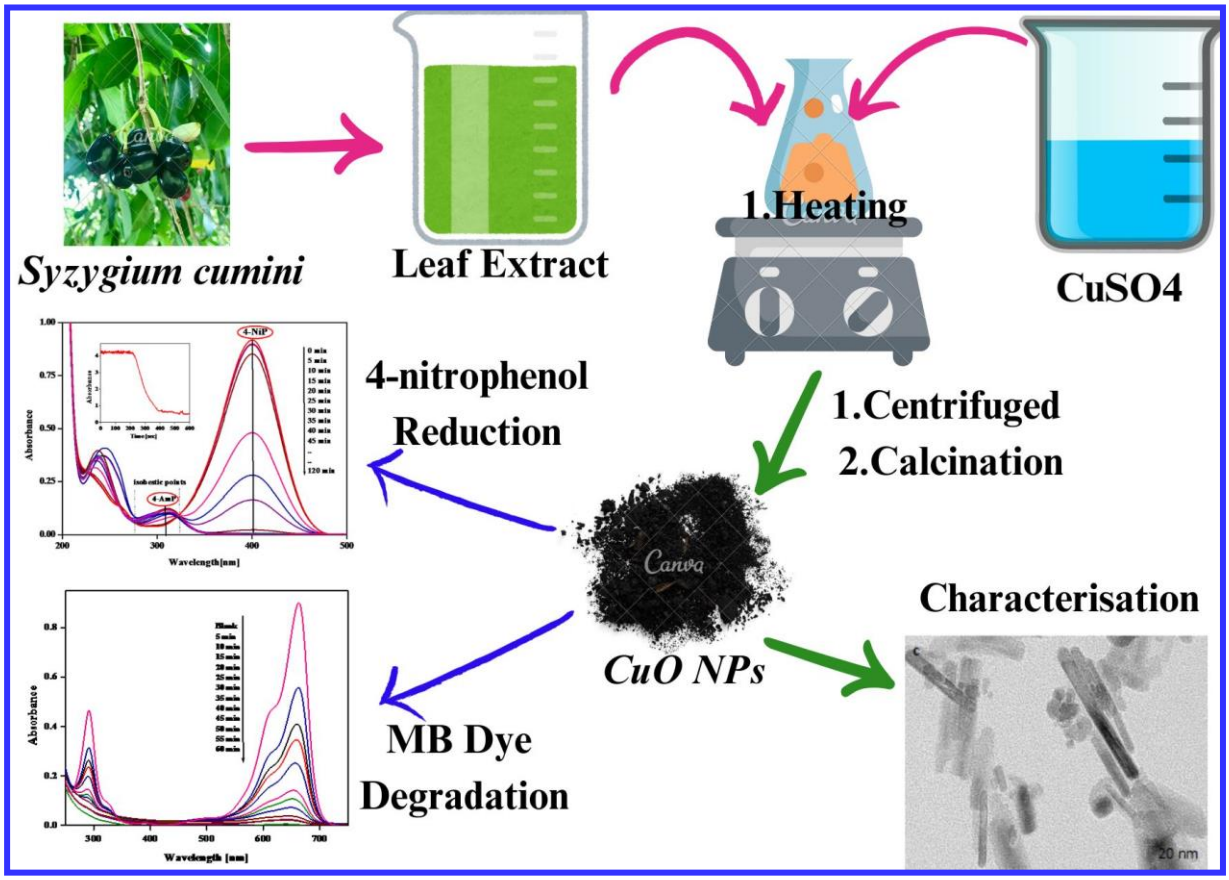

Advanced oxidation processes (AOPs) have been explored to completely eliminate organic pollutants, offering a promising solution to this challenge. Among these, semiconductor-based AOPs stand out as one of the most effective and cost-efficient options for tackling harmful dyes. These processes offer significant potential to harness the full solar spectrum in photocatalytic reactions [23]. AOPs use reactive free radicals to break down electron-rich dyes into harmless products like CO_2 and H_2O through mineralization process [23,24]. Various nanostructures have been investigated to develop efficient catalytic systems based on advanced oxidation processes (AOPs) [25–28]. Among these, metal oxide nanoparticles have emerged as one of the most effective approaches for the removal of pollutants from water [29–31]. Methylene blue (MB), a widely used cationic dye in rubber and plastic production, can be effectively degraded through photocatalysis using nanostructured semiconductor oxides [32].

4-Nitrophenol (4-Nip) is one of the most hazardous, toxic and anthropogenic pollutant extensively produced by industries. The discharge of 4-Nitrophenol from industries is detrimental and its removal is also a crucial task. The reduction of 4-Nitrophenol to 4-Aminophenol is an important reaction in pharmaceutical, pesticides, insecticides, natural products, plasticizers, explosives and dyes industries [33-34]. 4-nitrophenols are not reduced by $NaBH_4$ in aqueous or non-aqueous solutions, but this reaction easily occurs in presence of metals, particularly, coinage metals [35, 36], which are expensive. Therefore, it is essential to develop a low cost, ecofriendly catalyst for the reduction of 4-nitrophenol to 4-aminophenol in aqueous solution. *Syzygium cumini* L. (Myrtaceae) commonly known as Indian blackberry is native to Indonesia and is also found in Bangladesh, Algeria, India, Philippines, Brazil, Florida, Thailand, Israel and California. It contains variety of phytochemicals [37].

In this paper, we present a successful clean, reliable, biocompatible, cheap, and nontoxic green strategy to synthesize CuO NPs using *Syzygium cumini* leaf extract. The synthesized CuO nanoparticles, using Syzygium cumini as a bioreductant for the first time, effectively catalyzed the photodegradation of methylene blue under visible light. Their performance was also evaluated against CR, MO, and MG dyes, and in the reduction of 4-nitrophenol to 4-aminophenol under mild aqueous conditions.

MATERIALS AND METHODS

Materials

All chemicals used in the study were of AR grade and were used as received, without any further purification. Cupric sulphate pentahydrate ($CuSO_4.5H_2O$), methylene blue trihydrate (MB, $C_{16}H_{24}ClN_3O_3S$, mw: 373.896 g/mol, λ_{max} = 664 nm), malachite green oxalate (MG, $C_{52}H_{54}N_4O_{12}$, mw: 927.02 g/mol, λ_{max} = 616 nm), methyl orange (MO, $C_{14}H_{14}N_3NaO_3S$, mw: 327.334 g/mol, λ_{max} = 463 nm),congo red (CR, $C_{32}H_{22}N_6Na_2O_6S_2$, mw: 696.66 g/mol, λ_{max} = 498 nm) and hydrogen peroxide 30% by weight (99%) were purchased from Merck, Mumbai, India. 4-Nitrophenol (99.0%) and sodium borohydride (99.0%) were purchased from Sigma-Aldrich, USA.

Characterization

UV-visible and diffuse reflectance spectra were obtained using a JASCO V-650 spectrophotometer, while FT-IR spectra (4000–400 cm^{-1}) of the leaf extract and solid nanoparticles were recorded with a Thermo Scientific Nicolet iS5 spectrometer. Nanoparticle size and morphology were examined using a PHILIPS CM 200 TEM at 200 kV with 2.4 Å resolution. XRD patterns were recorded on a PANalytical X'Pert PRO diffractometer (model PW3071) using CuKα radiation (40 kV, 30 mA) over a 10°–80° 2θ range. Elemental composition was analyzed by EDX on a JEOL JED-2300 system. Nanoparticles were dispersed via an ultrasonic probe sonicator (Enertech ENUP-500A) for 30 one-minute cycles with 30-second intervals. Photocatalytic studies were performed in a Heber HIPR-MP-400 visible annular immersion photoreactor. Nanoparticles were separated using an Eltek refrigerated centrifuge (Model RC4100 F, max 15,000 rpm).

Methods

Fresh *Syzygium cumini* leaves (20 g), sourced from Nazareth, Tamil Nadu, were washed, chopped, and boiled in 100 mL of double-distilled water for 10 minutes. After cooling, the mixture was filtered (Whatman No. 41) to obtain a clear extract. For CuO nanoparticle synthesis, 10 mL of the extract (adjusted to pH 9 using 0.1 N NaOH) was mixed with 10 mL of 0.1 M cupric sulfate and heated for 10 minutes. A black colloidal suspension formed, which was centrifuged at 13,000 rpm, washed, dried at 110°C, and calcined at 500°C for 2 hours to yield CuO nanoparticles.

The photocatalytic performance of the synthesized CuO NPs was evaluated using methylene blue (MB) dye as a model pollutant. Experiments were conducted under both dark and visible light conditions, with and without H_2O_2. The pH of MB solutions was adjusted using 1.0 M H_2SO_4 or NaOH, and light intensity was varied from 150 W to 500 W [38, 39].

Photocatalytic Reduction of 4-nitrophenol in Alkaline Medium

In slightly alkaline medium (addition of $NaBH_4$ makes the solution slightly alkaline, (pH-9) the reduction of 4-Nip to 4-Amp by $NaBH_4$ in presence of CuO NPs as catalyst is fast even in the absence of light, and the reaction couldn't be investigated by conventional method. Hence the reaction was studied using the time course measurements mode in the spectrophotometer. In this mode, all the constituents were placed in the cuvette in the spectrophotometer and the reaction was initiated by adding required amount of the solid catalyst, and the reaction was followed by monitoring the absorbance with time at fixed wavelength. In highly alkaline medium (0.1 M NaOH or more), the reaction was moderately slow and $NaBH_4$ is reported to be highly stable. Under this condition, the reactions were performed by adding the desired amount of catalyst to pH adjusted (0.1 M NaOH) mixture of 4-nitrophenol and $NaBH_4$, and magnetically stirred in the photoreactor, while irradiating with visible light source. At predetermined time intervals during irradiation, 5 mL samples were collected, centrifuged at 10,000 rpm, and their absorbance was measured using a UV-Vis spectrophotometer. [40].

RESULTS AND DISCUSSION

Absorption Spectral Studies

The photo catalytic activity of a semiconductor is mainly due to the absorption of light and the migration of light induced electrons and holes, which depends upon the electronic structure of the materials. The UV-vis-DRS represented in the Fig.1a has absorption bands centered at 483 and 659 nm, due to d-d transitions are prime factors for the photocatalytic activity CuO NPs in the visible range [41]. The optical parameters such as absorption coefficient and band gap are resolved from the spectrum. From the Tauc plot, the band gap of CuO NPs is found to be 1.6 eV. The observed band gap value is greater than the bulk CuO NPs (1.2 eV) [35, 36], this is ascribed to the quantum effect of CuO NPs and the particle size was decreased [42].

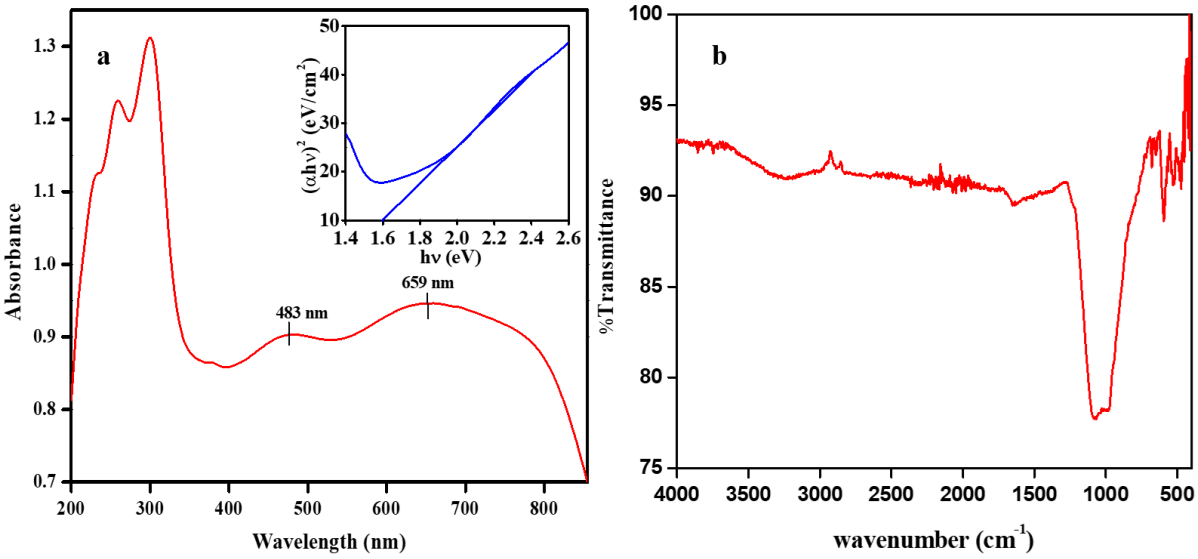

Figure 1. (a) UV-vis-Diffuse Reflectance spectrum of CuO NPs (Inset) Tauc plot (b) FT-IR spectrum of calcined CuO NPs.

FT-IR Spectra of CuO NPs

The FT-IR spectra of both as-prepared and calcined CuO nanoparticles are shown in Fig. 1b. A broad absorption band observed at 3458.62 cm^{-1} corresponds to the O–H stretching vibration, while the peak at 1620.92 cm^{-1} is attributed to the bending vibration of physically adsorbed water or surface hydroxyl groups. After calcination at 500 °C for one hour, distinct absorption peaks appear at 608, 512, and 471 cm^{-1}, which are characteristic of the asymmetric and symmetric stretching vibrations of Cu–O bonds, confirming the formation of CuO nanoparticles [43]. The absence of peaks associated with organic functional groups in the calcined sample indicates the removal of biomolecules initially present in the as-prepared sample, which were likely involved in the stabilization of the nanoparticles.

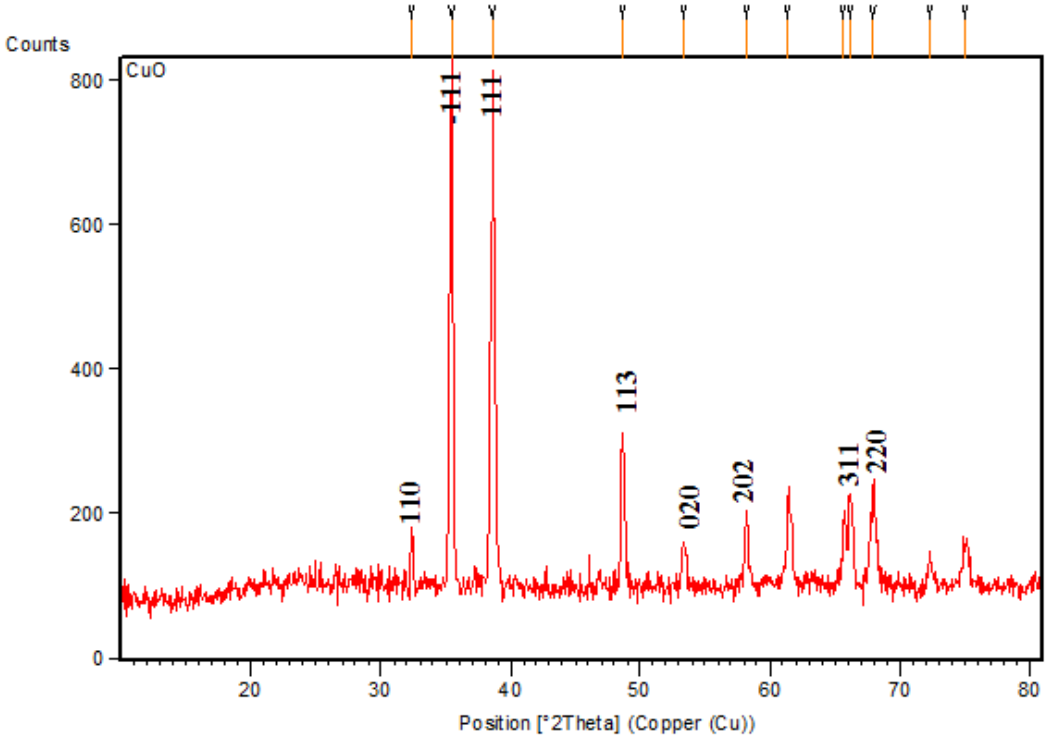

Figure 2. XRD of CuO NPs.

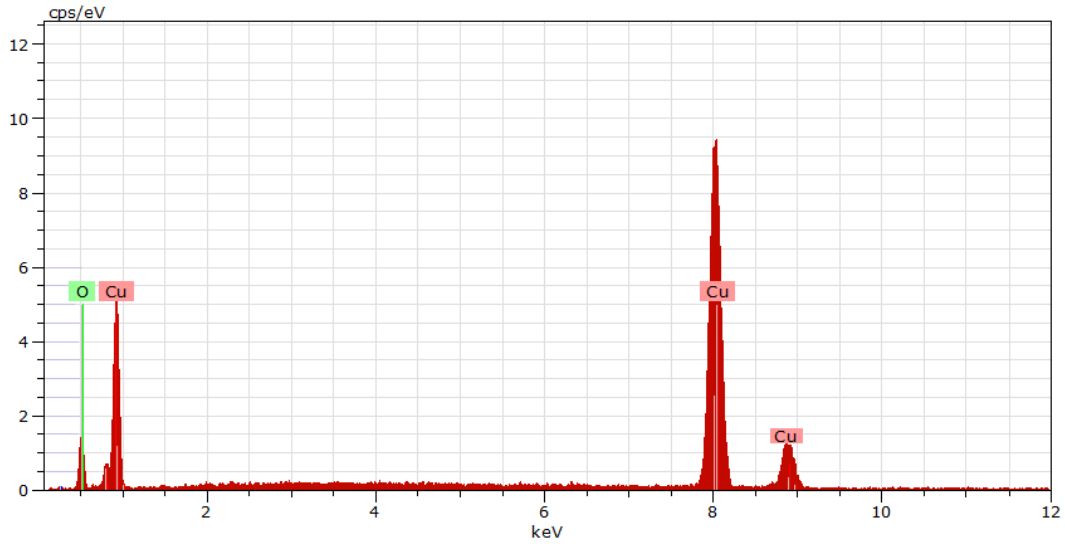

Figure 3. EDAX spectrum of CuO NPs.

XRD of CuO NPs

The formation of CuO nanoparticles was confirmed through X-ray diffraction (XRD) analysis, as shown in Fig. 2. The diffraction peaks observed at 2θ values of 32.29°, 35.43°, 38.58°, 43.66°, 48.9°, 53.39°, 58.23°, 61.39°, 66.13°, and 67.89° correspond to the (110), (−111), (111), (113), (020), (202), (311), and (220) crystallographic planes, respectively. These peaks are consistent with the monoclinic phase of CuO, as referenced by JCPDS card no. 72-0629 [44–45]. The absence of additional peaks related to Cu_2O or $Cu(OH)_2$ indicates the high phase purity of the synthesized nanoparticles. The average crystallite size, calculated using the Scherrer equation based on the most intense (−111) peak, was estimated to be approximately 34 nm

EDAX of CuO NPs

EDAX was performed on the synthesized copper oxide nanoparticles to determine their elemental composition. The EDAX spectrum Figure 3 is confirmed the presence of copper and oxygen as the only elemental constituents, verifying the successful formation of copper oxide nanoparticles. Characteristic peaks observed at 8 keV and 0.928 keV correspond to elemental copper [46]. The absence of any additional peaks in the spectrum further indicates the high purity of the CuO nanoparticles.

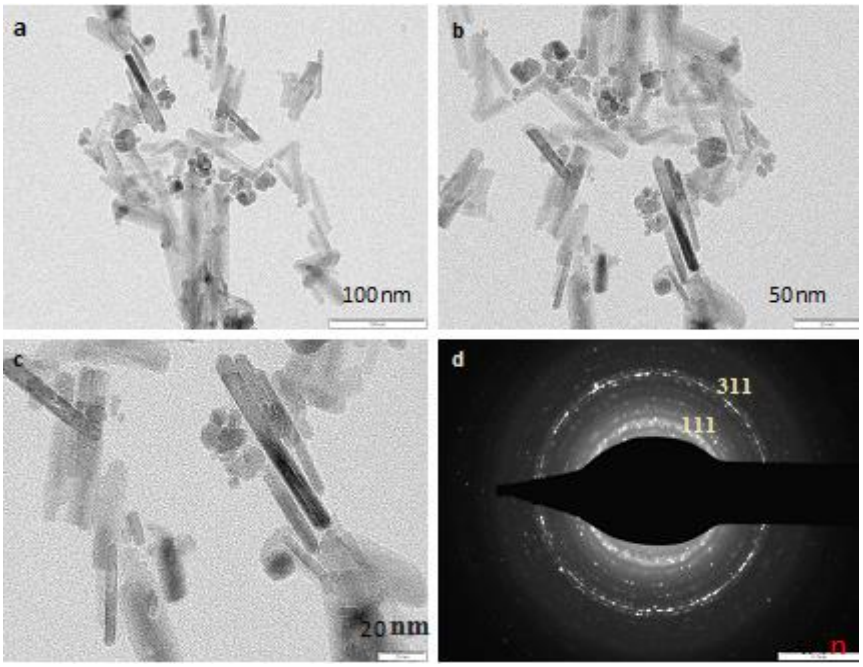

Figure 4. (a-d) TEM images of CuO nanoparticles.

TEM Studies of CuO NPs

TEM studies provided detailed insights into the shape, uniformity, and nanoscale features of the particles, confirming the structural integrity of the CuO NPs. Figure 4(a–d) presents the TEM images of CuO nanoparticles synthesized using *S. cumini* leaf extract. The images clearly show the formation of CuO nanorods with an average length of approximately 50 nm and a width of around 8 nm. As shown in Figure 4, it confirms the polycrystalline nature of the nanoparticles.

Photocatalytic Performance of CuO Nanoparticles

The catalytic efficiency of CuO NPs for the degradation of MB in presence of H_2O_2 was studied under different experimental conditions (Fig 5). Dye removal using a photocatalyst typically involves a combination of adsorption and photocatalytic degradation. To account for any adsorption effects, CuO nanoparticles were first equilibrated with the dye solution under dark conditions for 30 minutes. This step ensured that adsorption-desorption equilibrium was achieved prior to photocatalytic testing. After equilibrium was reached, the reaction mixture was exposed to artificial visible light, and the kinetics of photocatalytic degradation were subsequently investigated. In the dark (without radiation), the CuO NPs have limited effect, the intensity of the dye is decreased to an extent of 11.86%, but on exposure to visible light source of 500 W, almost 100% degradation is noticed [47].

Impact of Reaction Parameters on the Degradation of MB

The experimental results at varying initial concentrations of methylene blue (1×10^{-5} M to 5×10^{-5} M), by keeping H_2O_2 concentration, CuO NPs dosage and the visible light source as constant are shown in Figure 6a-d [48,49].

As the initial concentration of MB increased (1×10^{-5} M to 5×10^{-5} M), the degradation efficiency decreased. Higher MB concentrations absorb more incident light, reducing light availability for photocatalyst activation. Additionally, excess MB molecules block active sites on the CuO surface, hindering further adsorption and reactive species formation.

Degradation improved with increasing pH. Alkaline conditions promote the formation of hydroxyl radicals (•OH) due to an increase in OH^- ions, which are critical for photocatalytic activity. MB, being positively charged, adsorbs better in basic conditions, enhancing degradation [50,51]. Higher H_2O_2 concentrations boosted degradation efficiency. H_2O_2 acts as an electron acceptor, generating additional •OH radicals upon reaction with photoexcited electrons, which actively degrade MB molecules [52].

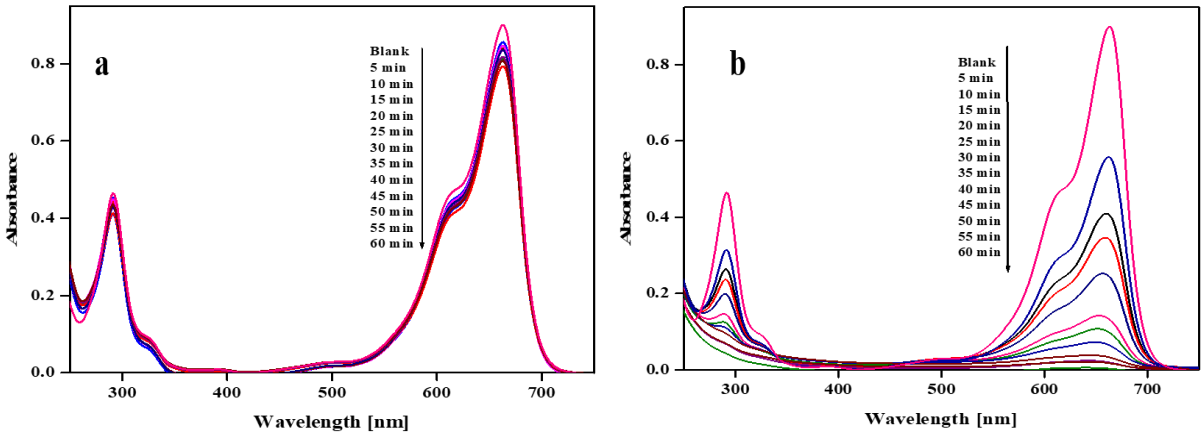

Figure 5. UV-visible spectra (time dependent) for degradation of MB with CuO NPs (a) under dark condition, (b) under visible light irradiation ($[H_2O_2] = 5\times10^{-3}$ M, $[MB] = 1\times10^{-5}$ M, CuO NPs = 5 mg/50 mL, pH = 6, Light source = 500 W).

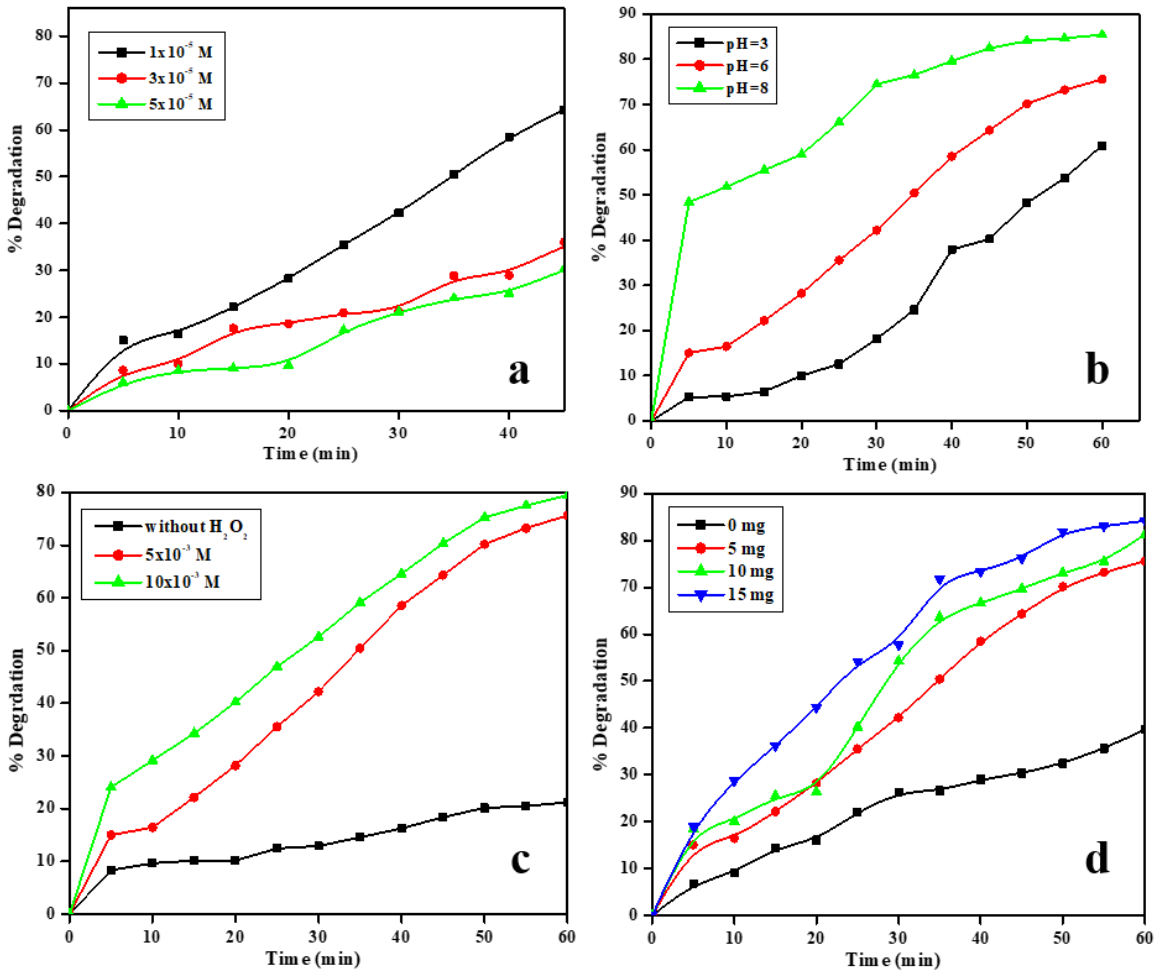

Figure 6. Effect of reaction parameters on the degradation of MB (a) Concentration of MB, (b) pH, (c) Concentration of H_2O_2 and (d) Catalyst dosage (Fixed parameters [MB] = 1×10^{-5} M, [H_2O_2] = 5×10^{-3} M, CuO = 5 mg/50 mL, pH = 6, Light source = 150 W).

Increasing CuO NP dosage (5–15 mg) led to improved degradation due to the availability of more active sites, resulting in enhanced generation of reactive species under light exposure [53]. Degradation efficiency rose with light intensity, (Figure 7) as more photons striking the CuO surface increased electron excitation, promoting the formation of reactive species essential for MB breakdown [54].

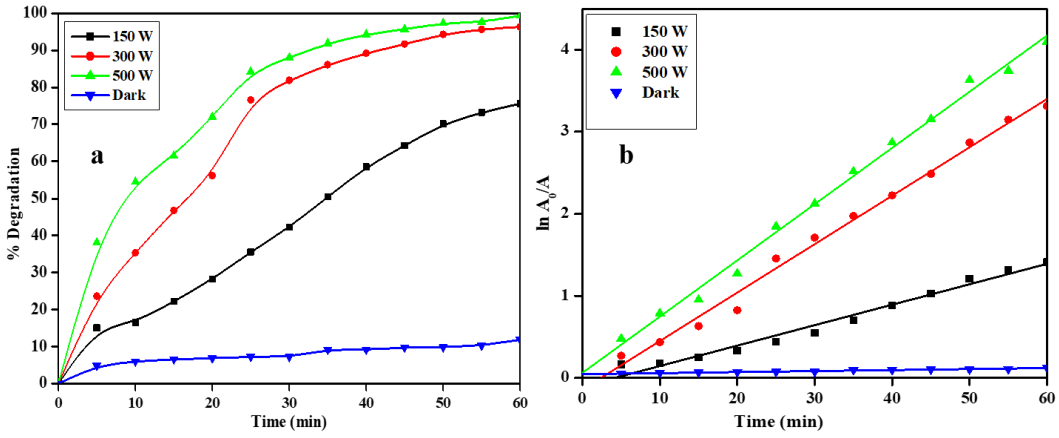

Figure 7. (a) Effect of visible light source on degradation, (b) Plot of ln(A_0/A) Vs Time in the degradation of MB by CuO NPs at different intensities of visible light ([MB] = 10µM, [H_2O_2] = 5×10^{-3} M, CuO NPs = 5 mg/50 mL, pH = 6).

Table 1. Rate constants for the degradation MB by CuO NPs under different conditions.

Condition		k, min^{-1}
[MB] (M)	1×10^{-5}	0.0205
	3×10^{-5}	0.0073
	5×10^{-5}	0.0072
pH	3	0.0164
	6	0.0249
	8	0.0260
$[H_2O_2]$ (M)	Without H_2O_2	0.0029
	5×10^{-3}	0.0249
	10×10^{-3}	0.0254
Catalyst Dosage (mg)	0	0.0075
	5	0.0249
	10	0.0282
	15	0.0321
Light source (W)	Dark	0.0012
	150	0.0249
	300	0.0590
	500	0.0685

Photocatalytic Degradation Kinetics of MB using CuO NPs.

The first-order rate constant (kapp) was calculated from the slopes of the linear plots using L-H model for the degradation of MB, as shown in Table 1.

Mechanism of Photocatalytic Degradation of MB by CuO NPs

The photocatalytic degradation of dyes by CuO nanoparticles follows semiconductor mechanism. In the above mechanism, upon irradiation the semiconductor nanoparticles produces photoexited electrons and the valence band has holes. These excited electrons combones with the water molecule and produces reactive oxygen species. The addition of H_2O_2 favours the formation of reactive oxygen species and attack the dye molecule subsequently degrade them into smaller molecules which are non toxic [55].

Stability and Recyclability

The stability of CuO nanoparticles towards the photodegradation of dyes and its recyclability were presented in Figure 8. For this, the experiments were carried out for 60 minutes following the same conditions with the same catalyst. After each cycle, the catalyst was recovered through centrifugation and then rinsed with water and ethanol. Then the catalyst was dried for about one hour at 60°C. The results of the study shows that 98% degradation of MB dye is achieved in 60 min. So, there is no loss of photocatalytic activity in all repeated cycleswith similar apparent rate constant values [56].

The results confirm the stability of the CuO nanoparticles, as their photocatalytic properties remained unaffected after repeated use. The simplified recycling process (centrifugation and mild drying) demonstrates its practical potential for industrial applications, lowering operational costs and minimizing waste. The consistent values show that the catalyst's active sites stay intact, preventing typical problems such as agglomeration or surface poisoning. The catalyst's reliable performance under these conditions underscores its robustness.

Degradation of Different Dyes by CuO NPs

Various types of dyes, including the positively charged methylene blue (MB) and malachite green (MG), as well as the negatively charged methyl orange (MO) and Congo red (CR), were used as target dyes to evaluate the photocatalytic performance of the synthesized CuO nanoparticles. This selection of dyes allowed for a comprehensive assessment of the CuO NPs' ability to degrade different dye molecules with varying charge characteristics. Under the same reaction conditions, the removal efficiencies for MG, CR and MO are 31.47 % 53.02% and 14.04% after irradiation of 40 min respectively (Figure 9d). The apparent rate constant calculated from the slopes are 2.42×10^{-2} min^{-1} (MB), 1.40×10^{-2} min^{-1} (MG), 2.31×10^{-2} min^{-1} (CR) and 0.05×10^{-2} min^{-1} (MO The experimental results show that the as-synthesized CuO NPs exhibit selective dye degradation, with notably higher photocatalytic efficiency for CR and MB [57].

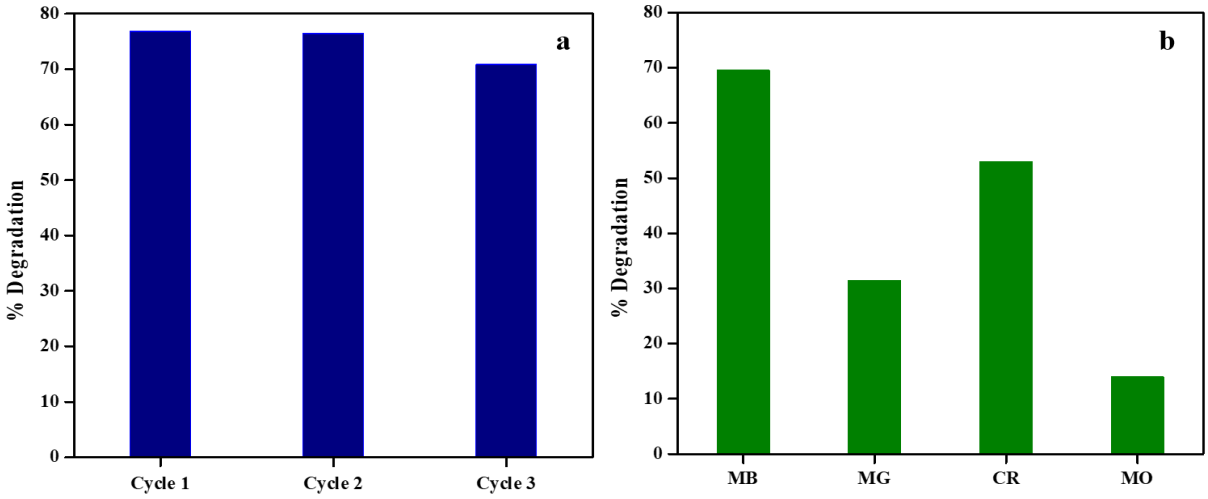

Figure 8. (a) Stability and reusability of CuO NPs (b) Comparison of CuO NPs for the degradation of various dyes. ([Dye] = 10μM, $[H_2O_2] = 5\times10^{-3}$ M, CuO NPs = 5 mg/50 mL, pH = 6, Light source = 150 W).

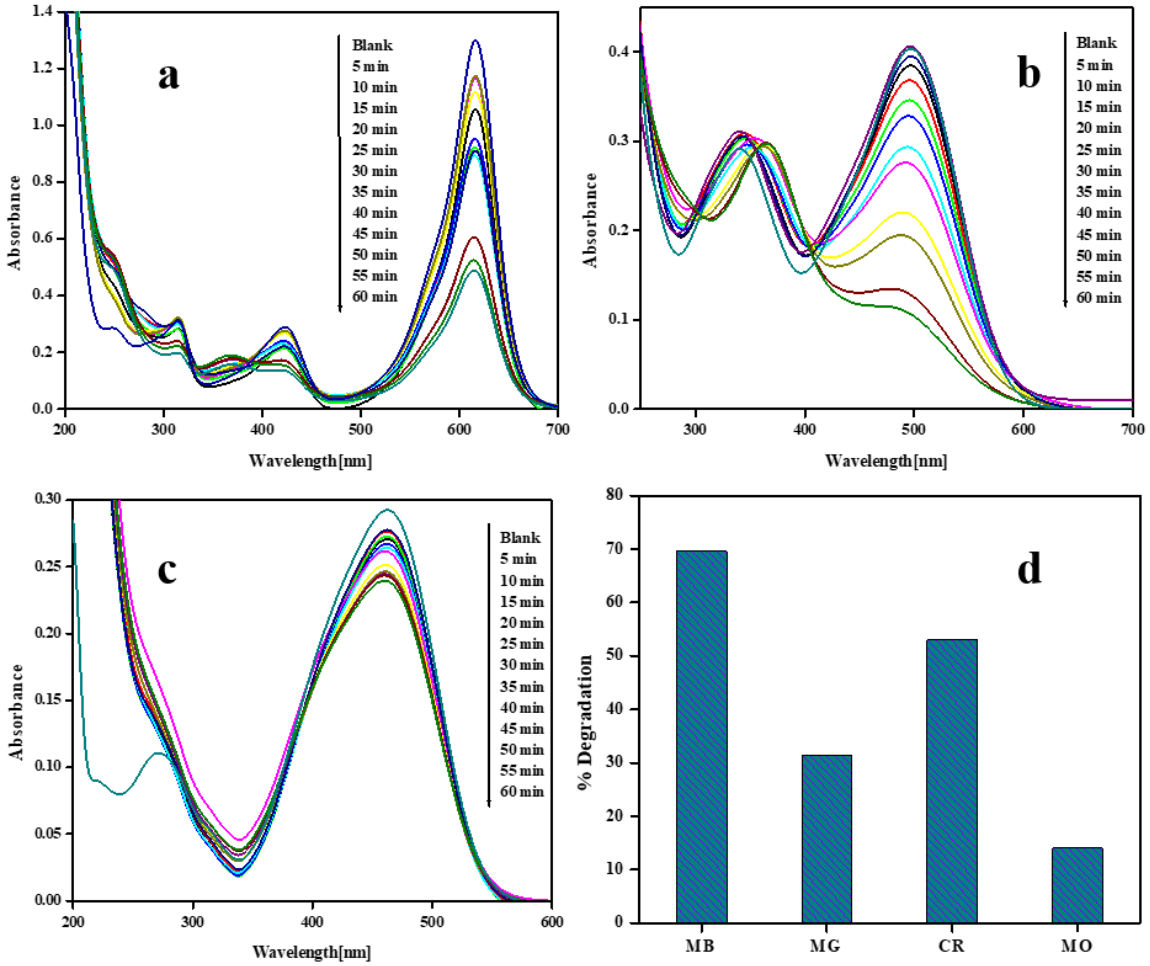

Figure 9. UV-vis absorption spectra (time-dependent) for the degradation of (a) MG (b) CR & (c) MO with CuO NPs (d) Comparison of CuO NPs for the degradation of MG, CR and MO ([Dye] = 10μ M, $[H_2O_2] = 5\times10^{-3}$ M, CuO NPs = 5 mg/50 mL, pH = 6, Light source = 150 W).

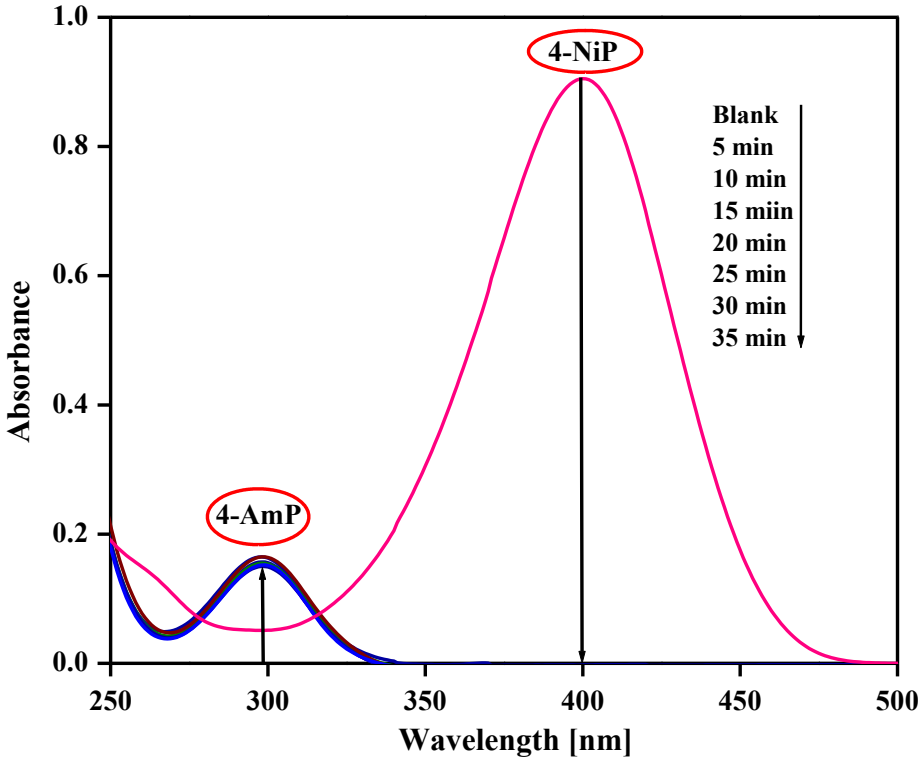

Figure 10. Time dependent UV-visible spectra for reduction of 4-Nip by $NaBH_4$ in presence of CuO NPs as a catalyst, (In absence of visible light irradiation) ([4-Nip]= 5×10^{-4} M, [$NaBH_4$]= 0.05 M, CuO NPs = 10 mg/50 mL).

Catalytic Conversion of 4-nitrophenol to 4-aminophenol

The reduction of 4-nitrophenol (4-Nip, E^o = –0.76 V) to 4-aminophenol (4-Amp) is thermodynamically favorable using $NaBH_4$ (E^o = –1.33 V) under ambient conditions. While noble metal nanoparticles like Ag, Au, and Cu have been widely used as catalysts, this study explores the catalytic efficiency of bio-derived CuO nanoparticles. [58] In aqueous solution, 4-Nip shows an absorption peak at 317 nm, which shifts to 400 nm upon $NaBH_4$ addition due to increased alkalinity. Without the catalyst, no reduction occurs. Upon introducing CuO NPs, the 400 nm peak decreases and a new peak at ~300 nm appears, confirming the formation of 4-Amp (Figure 10).

The catalytic reduction of 4-nitrophenol (4-Nip) to 4-aminophenol (4-Amp) using CuO nanoparticles was confirmed by UV-visible spectroscopy. An isobestic point in the spectra indicates a clean conversion with no side reactions. As the reaction proceeds, the absorbance peak of 4-Nip diminishes, confirming complete reduction. The reaction was studied under pseudo-first-order conditions, with $NaBH_4$ in large excess to maintain a constant concentration and suppress aerial oxidation of the product. [61] The concentrations of 4-Nip tested were 5×10^{-4} M, 10×10^{-4} M, and 15×10^{-4} M, while $NaBH_4$ concentrations were varied from 0.05 M to 1.5 M. CuO nanoparticle dosage was fixed at 10 mg per 50 mL.

Among the tested conditions, the combination of [4-Nip] = 5×10^{-4} M and [$NaBH_4$] = 0.05 M exhibited the highest catalytic activity. The reaction was monitored in real-time using a UV-Vis spectrophotometer. In a typical experiment, 1.5 mL of 5×10^{-4} M 4-Nip was mixed with 1.5 mL of 0.05 M freshly prepared $NaBH_4$ in a quartz cuvette. Then, 2 mg of CuO NPs was added, and the reaction was tracked by observing the color change from yellow to colorless. The reduction was completed within ~120 seconds, as shown in Figure 11.

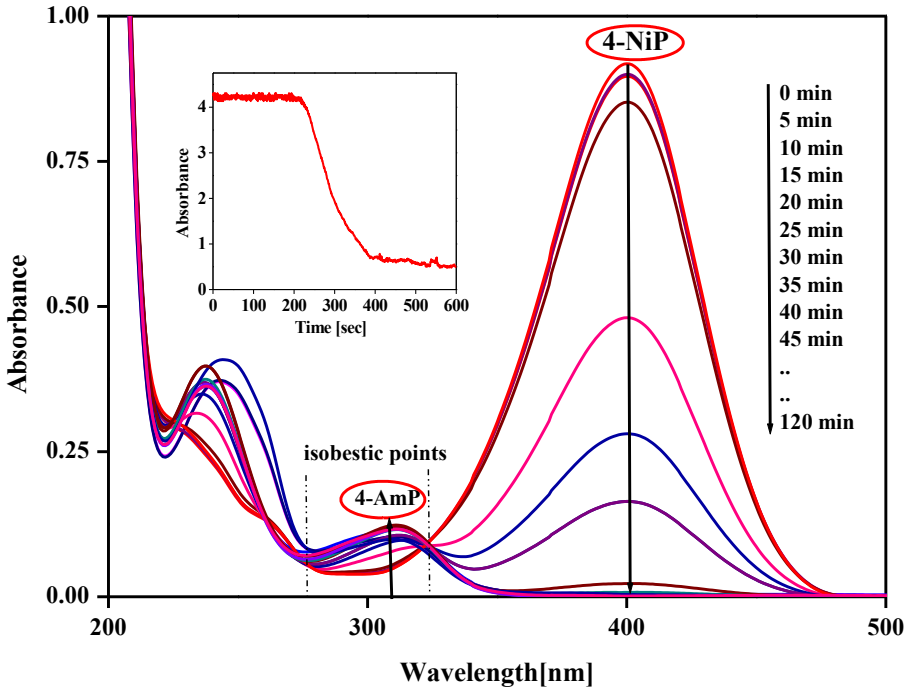

Figure 11. (a) Time course measurement spectra for catalytic reduction of 4-Nip by $NaBH_4$(a) CuO NPs ([4-Nip] = 1×10^{-3} M, [$NaBH_4$] = 0.025 M, CuO NPs = 3 mg/3 mL of reaction mixture)(b) Time dependent UV-visible spectra for reduction of 4-Nip by $NaBH_4$ in presence of CuO nanoparticles in alkaline conditions under visible light irradiation ([4-Nip]= 5×10^{-4} M, [$NaBH_4$]= 0.05 M, CuO NPs = 10 mg/50 mL, Light source = 500 W).

But when the $NaBH_4$ solution prepared in 0.1 M NaOH is used, the reaction was slow and could be comfortably studied. The system shows an induction period for about 15 min and after that the catalytic reduction starts. From the Figure 11b it is clear that up to 15 min there is a slight decrease in absorption, which may due to adsorption of the 4-nitrophenolate anion over the catalyst. After that a sudden decrease in absorption is noticed due to catalytic reduction and the reaction proceeds smoothly. The induction period is reported in the 4-Nip reduction using $NaBH_4$ in various literatures. The main reasons attributed are the time required for the reducing agent to inject electrons into the metal and slow diffusion of reactants to the surface of the nanoparticles [62]. To evaluate the rate constants, the Langmuir–Hinshelwood apparent first-order kinetics model is applied. In this mechanism, the reduction occurs via electron transfer from the donor species, BH_4^- (hydride ion), to the acceptor, 4-nitrophenol (4-Nip). The reaction kinetics equation can be described with the equation and the rate constant is calculated from the slope of the plot.

$$(dC_t/dt) = -k_{app}\,t \quad \text{or} \quad \ln(C_t/C_0) = \ln(A_0/A_t) = k_{app}\,t$$

The reduction of 4-nitrophenol (4-NP) using CuO nanoparticles was studied under various conditions. Increasing the initial concentration of 4-NP led to a decrease in the rate constant due to surface saturation of the catalyst, limiting BH_4^- adsorption and electron transfer—consistent with the Langmuir-Hinshelwood mechanism. In contrast, variations in $NaBH_4$ concentration had negligible impact, as it was used in large excess [63,64]. An increase in catalyst dosage significantly enhanced the reaction rate by providing more active sites for adsorption and reduction. Similarly, higher visible light intensity improved the reaction rate by promoting electron excitation, which accelerated the reduction process. Table 2 compares CuO NPs synthesized from different natural sources and their efficiency in degrading various dyes. The data confirm that CuO NPs synthesized in this study exhibit superior and more consistent performance, especially under optimized conditions involving visible light and excess $NaBH_4$ [65,66].

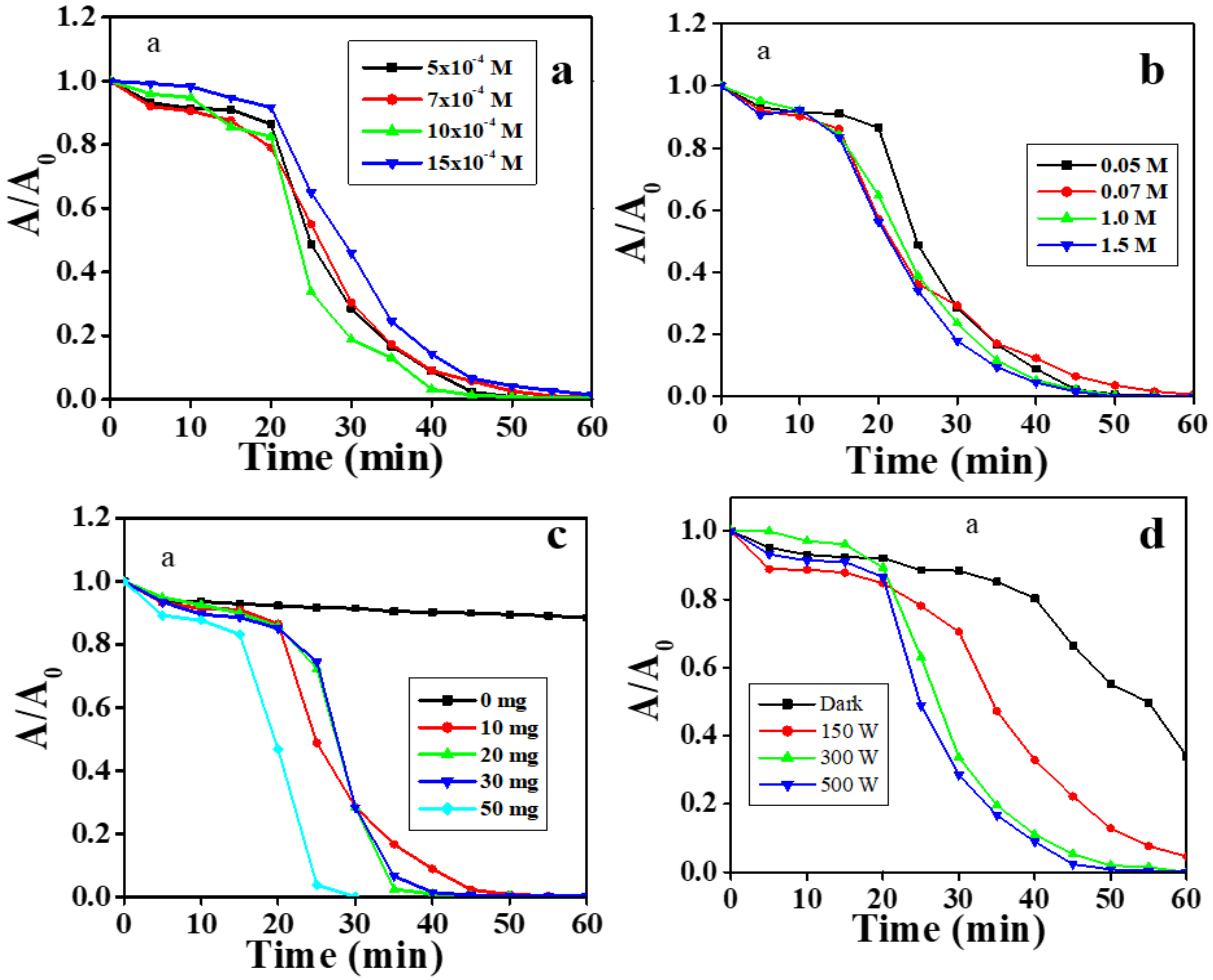

Figure 12. Effect of reaction parameters on the catalytic reduction of 4-nitrophenol to 4-aminophenol (a) Concentration of 4-NiP, (b) $NaBH_4$, (c) Catalyst dosage and (d) Intensity of light.

Table 2. Comparison of dye degradation potential of CuO NPs.

Source	Dye	Conc. CuO / Dye, M	Condition	% Degradation	Time/rate constant, min^{-1}	Ref.
Ferulago angulate	Rh B	50 mg/50 mL/ $1x10^{-4}$µM	Visible light, stirring, RT	83% (150 min)		[1]
Rosmarinic acid	MB	0.1 mg of CuO NPs 3 mL of 3.12 x 10^4 M MB	excess NaBH4	12 min		[2]
Psidium guajava	Nile blue Reactive yellow 160	10 mg/20 mL dye NB- $1.3x10^{-5}$ M RY- $4.8x10^{-5}$ M (40 ppm both)	Sunlight, stirring,	93% (120 min) 81% (120 min)	0.023 0.014	[3]
Carica papaya	Coomassie brilliant blue R250	10 mg/ 50 ml dye (10 mg/L)	Sunlight, stirring	~37% (90 min)	-	[4]
Citrus aurantifolia	Rhodamine B	CuO 10 ppm Dye 10 ppm	UV light	91% (120 min)	~0.087	[5]
Acalypha Indica	MB	CuO 20 mg/50 mL/ L MB	Visible light 400 W Xe lamp	75% CuO 83.2% GO-CuO	60 min	[6]

Punica granatum	MB	25 mg/25 mL dye MB 50mg/L	Adsorption, shaking 120 rpm, 298 K	92.2% q_e - 46.84 mg/g	240 min	[7]
Melissa officinalis	RhB	CuO 5mg /50 mL RhB 2x 10^{-5} M		~100%	10 min	[8]
Euphorbia maculata	MB CR RhB	CuO 50mg /50 mL Dye 10mg/mL	UV light with stirring	96% 85 89%	-	[9]
Rheum palmatum root	MB RhB	MB 3.1×10^{-5} M RhB 2.1×10^{-3} M	$NaBH_4$ (5.3 $\times$ 10^{-3} M, 25 mL) CuO NPs/clinoptilolite	~100%	60 s	[10]
Psidium guajava	MB MO MR EY	1mL of 1 mg/10 mL aqueous solution 1 x 10^{-4} M dye	$NaBH_4$ (1x 10^{-3} M) stirring	91% (12 min) 80% (4 min) 89% (4 min) 97% (4 min)	0.419min^{-1} 0.734min^{-1} 0.789min^{-1} 1.601min^{-1}	[11]
L-lysine	MB EY	10 mg/200 mL 1x 10^{-4} M		97% 180 min 99.1% 40 min	0.021min^{-1} 0.105min^{-1}	[12]
Ruellia tuberosa	Crystal violet	10 mg/L	Sunlight, stirring	~100% 120 min	-	[13]
Curcumin	MB	1 mg/mL CuO NPs 10 µg/mL MB Total volume 3mL.	200 µl of 0.5 mg/mL of NaBH4, 800 rpm	27 min	0.04629 min^{-1}	[14]
Cystoseira trinodis	MB	50 mg/100 mL 5ppm	UV Sunlight	89% 150 min 87% 150 min		[15]

Table 3. Comparison of 4-nitrophenol reduction potential of CuO NPs.

Source of CuO NPs	Conc. of 4-NP/CuO	% Conversion/ Condition	Time/Rate constant	Ref
Theobroma cacao	2.5 x 10^{-3} M/ 7 mg/50 mL	~100% Pd/CuO	0.055 s^{-1}	[1]
Melissa Officinalis L.	2.5 x 10^{-3} M/ 5 mg/50 mL	Stirring	22 min	[2]
Gundelia tournefortii	2.5 x 10^{-3} M/ 10 mg/50 mL	-	0.045 s^{-1}	[3]
Murayya koeniggi	5.0 x10^{-5} M/ 1 mg/3mL	95.8% Quartz cuvette	9.2 x 10^{-3} s^{-1}	[4]
Euphorbia chamaesyce	2.5 x 10^{-4} M/ 7 mg/50 mL	100%	3 min	[5]
Tecoma castan	2.5 x 10^{-3} M/ 10 mg/3 mL	$NaBH_4$ Quartz cuvette	0.18 min^{-1}	[6]
Rheum palmatum L.	2.5 x 10^{-3} M/ 7 mg/50 mL	$NaBH_4$ stirring	2.5 min	[7]
Rosehip fruits	10 ppm/ 100 mg/50 mL	88% H_2O_2	150 min	[8]
Psidium guajava	5 x 10^{-5} M/ 1mL of 1 mg/10 mL aqueous solution	99%, $NaBH_4$ stirring	6 min, 0.261 min^{-1}	[9]

L-lysine	60µl of 0.006M/ 300µl aq. sol. of CuO NPs (0.001g)	300µl of 0.1M $NaBH_4$ Quartz cuvette	6 min 0.403 min^{-1}	[10]
Chemical method	$2.5x10^{-3}$ M CuO 50 mg/L CuO@Ag^0 50 mg/L	90% Quartz cuvette	0.082 min^{-1} (10 min) 0.118 min^{-1} (5 min)	[11]
Ranolazine	$1x10^{-4}$ M 0.5 mg/mL CuO NPs	99% 10 mM $NaBH_4$ Quartz cuvette	8.8 $x10^{-3}$ s^{-1} 320 s	[12]
Rosmarinic acid	200 µL of 100 mM NP 0.1 mg of CuO NPs	excess NaBH4 Polystyrene cuvette	10 min	[13]

The Table 3. reflects the effectiveness of CuO NPs synthesized from various natural sources in reducing 4-nitrophenol. The reduction efficiency is influenced by factors such as the source of CuO NPs, concentration of reactants, use of $NaBH_4$, and reaction conditions like stirring or light exposure. Our work is noteworthy for their rapid and complete reduction potential, demonstrating high efficacy in 4-NP reduction.

CONCLUSION

The photocatalytic reduction of 4-nitrophenol and degradation of methylene blue (MB) dye using green-synthesized CuO nanoparticles (NPs) has demonstrated their high catalytic efficiency and environmental relevance. Under visible light irradiation for 60 minutes, the CuO NPs achieved a remarkable 98% degradation of MB dye, indicating their strong potential for wastewater treatment applications. Additionally, the rapid reduction of 4-nitrophenol to 4-aminophenol within just five seconds further highlights the nanoparticles' excellent catalytic properties. The reusability of the catalyst was also evaluated, showing consistent performance over three cycles without significant loss in activity, thereby confirming its durability and sustainability for long-term use.These results underscore the effectiveness of the eco-friendly synthesis route employing Syzygium cumini leaf extract. However, the study lacks detailed investigation into the underlying photocatalytic mechanisms, such as reactive oxygen species (ROS) generation, charge transfer pathways, and the role of specific phytochemicals in enhancing catalytic activity. Addressing these aspects could provide a deeper understanding of the material's performance. Future research should also explore the scalability of the synthesis process and test the catalyst under real environmental conditions, including natural sunlight and actual industrial effluents. Overall, this green approach to CuO NP synthesis presents a promising strategy for sustainable catalysis and environmental remediation.

ACKNOWLEDGEMENTS

The authors sincerely thank the Management and Principal of V.O. Chidambaram College, Tuticorin, as well as the Head and faculty of the Department of Chemistry, for their constant encouragement and the provision of research facilities.

REFERENCES

1. Sukumar, S., Rudrasenan, A. and Nambiar, D. P. (2020) Green-Synthesized Rice-Shaped Copper Oxide Nanoparticles Using *Caesalpinia bonducella* Seed Extract and Their Applications. *ACS Omega*, **5**, 1040–1051.

2. Wang, F., Li, H., Yuan, H., Sun, Y., Chang, F., Deng, H., Xie, L. and Li, A. (2016) A highly sensitive gas sensor based on CuO nanoparticles synthetized via a sol–gel method. *RSC advances*, **6**, 79343–79349.

3. Akbari, A., Amini, M., Tarassoli, A., Eftekhari-sis, B., Ghasemian, N. and Jabbari, E. (2018) Transition metal oxide nanoparticles as efficient catalysts in oxidation reactions. *Nano-Structures & Nano-Objects*, **14**, 19–48.

4. Baqer, A. A., Matori, K. A., Al-Hada, N. M., Kamari, H. M., Shaari, A. H., Saion, E. and Chyi, J. L. Y. (2018) Copper oxide nanoparticles synthesized by a heat treatment approach with structural, morphological and optical characteristics. *Journal of Materials Science: Materials in Electronics*, **29**, 1025–1033.

5. Jadhav, M. S., Kulkarni, S., Raikar, P., Barretto, D. A., Vootla, S. K. and Raikar, U. S. (2018) Green biosynthesis of CuO & Ag–CuO nano-particles from Malusdomestica leaf extract and evaluation of antibacterial, antioxidant and DNA cleavage activities. *New Journal of Chemistry*, **42**, 204–213.

6. Mallakpour, S., Azadi, E. and Hussain, C. M. (2020) Environmentally benign production of cupric oxide nanoparticles and various utilizations of their polymeric hybrids in different technologies. *Coordination Chemistry Reviews*, **419**, 213378.

7. Singh, J., Kumar, V., Kim, K. H. and Rawata, M. (2019) Biogenic synthesis of copper oxide nanoparticles using plant extract and its prodigious potential for photocatalytic degradation of dye. *Environment*, **177**, 108569.

8. Prakash, S., Alagesan, N. E., Venkatesan, Subashini, K., Sowndharya, M. and Sujatha, V. (2018) Green synthesis of copper oxide nanoparticles and its effective applications in Biginelli reaction, BTB photodegradation and antibacterial activity. *Advanced Powder Technology*, **29**, 3315–3326.

9. Qasem, M., Kurdi, R. E. and Patra, D. (2020) Green Synthesis of Curcumin Conjugated CuO Nanoparticles for Catalytic Reduction of Methylene Blue. *Chemistry Select*, **5**, 1694 –1704.

10. Alinezhad, H. and Pakzad, K. (2019) C-S cross-coupling reaction using novel and green synthesized CuO nanoparticles assisted by *Euphorbia maculata* extract. *Applied Organo metalic Chemistry*, **33**, e5144.

11. Hosseinzadeh, R., Mohadjerani, M. and Mesgar, S. (2017) Green synthesis of copper oxide nanoparticles using aqueous extract of Convolvulus percicus L. as reusable catalysts in cross-coupling reactions and their antibacterial activity. *IET Nanobiotechnolgy*, **11**, 725–730.

12. Sasidharan, D., Namitha, T. R., Johnson, S. P., Jose, V. and Mathew, P. (2020) Synthesis of silver and copper oxide nanoparticles using *Myristica fragrans* fruit extract: Antimicrobial and catalytic applications. *Sustainable Chemistry and Pharmacy*, **16**, 100255.

13. Jadhav, M., Kulkarni, S., Raikar, P., Barretto, D. A., Vootla, S. K. and Raikar, U. S. (2018) Green Biosynthesis of CuO & Ag-CuO nanoparticles from *Malus Domestica* leaf extract and evaluation of antibacterial, antioxidant, DNA cleavage activities. *New Journal of Chemistry*, **42**, 204–213.

14. Oza, F., Calzadilla-Avila, A. I., Calderon, A. R., Anna, K. K., Bon, R. R., Ramirez, J. T. and Sharma, A. (2019) pH-dependent biosynthesis of copper oxide nanoparticles using Galphimia glauca for their cytocompatibility evaluation. *Applied Nanoscience*, **10**, 541–550.

15. Sarkar, J., Chakraborty, N., Chatterjee, A., Bhattacharjee, A., Dasgupta, D. and Acharya, N. (2020) Green Synthesized Copper Oxide Nanoparticles Ameliorate Defence and Antioxidant Enzymes in Lens culinaris. *Nanomaterials*, **10**, 312.

16. Hemmati, S., Mehrazin, L., Hekmati, M., Izadi, M. and Veisi, H. (2018) Biosynthesis of CuO nanoparticles using *Rosa canina* fruit extract as a recyclable and heterogeneous nanocatalyst for C-N Ullmann coupling reactions. *Materials Chemistry and Physics*, **214**, 527–532.

17. Jiang, T., Poyraz, A. S., Iyer, A., Zhang, Y., Luo, A., Zhong, W., Miao, R., Sawy, A. M. E., Guild, C. Z., Sun, Y., Kriz, D. A. and Suib, S. L. (2015) Synthesis of Mesoporous Iron Oxides by an Inverse Micelle Method and Their Application in the Degradation of Orange II under Visible Light at Neutral Ph. *The Journal of Physical Chemistry*, **119**, 10454–10468.

18. Islam, M. R. and Mostafa, M. G. (2018) Textile Dyeing Effluents and Environment Concerns - A Review. *Journal of Environmental Science and Natural Resources*, **11**, 131–144.

19. Singh, J., Kumar, V., Kim, K. H. and Rawat, M. (2019) Biogenic synthesis of copper oxide nanoparticles using plant extract and its prodigious potential for photocatalytic degradation of dyes. *Environmental Research*, **177**, 108569.

20. Lavanya, C. (2014) Review article degradation of toxic Dyes: a review. *International Journal of Current Microbiology and Applied Sciences*, **3**, 189–199.

21. Khandelwal, M., Choudhary, S., Harish, Kumawat, A., Misra, K. P., Khangarot, R. K. and Rathore, D. S. (2023) *Asterarcys Quadricellulare* algae-mediated copper oxide nanoparticles as a robust and recyclable catalyst for the degradation of noxious dyes from waste water. *RSC Advances*, **13**, 28179.

22. Aroob, S., Carabineiro, S. A. C., Taj, M. B., Bibi, I., Raheel, A., Javed, T., Yahya, R., Alelwani, W., Verpoort, E. and Kamwilaisak, K. (2023) Green Synthesis and Photocatalytic Dye Degradation Activity of CuO Nanoparticles. *Catalysts*, **13**, 502.

23. Bahrami, M. and Ejhieh, A. N. (2015) Effect of the supported ZnO on clinoptilolitenano-particles in the photodecolorization of semi-real sample bromothymol blue aqueous solution. *Materials Science in Semiconductor Processing*, **30**, 275-284.

24. Jayasimha, H. N., Chandrappa, K. G., Sanaull, P. F. and Dileepkumar, V. G. (2024) Green synthesis of CuO nanoparticles: A promising material for photocatalysis and electrochemical sensor. *Sensors International*, **5**, 100254.

25. Ajoudanian, N. and Ejhieh, A. N. (2015) Enhanced photocatalytic activity of nickel oxide supported on clinoptilolite nanoparticles for the photodegradation of aqueous cephalexin. *Materials Science in Semiconductor Processing*, **36**, 162–169.

26. Anjum, F., Shaban, M., Ismail, M., Gul, S., Bakhsh, E. M., Ali Khan, M., Sharafat, U., Bahadar Khan, S. Khan, M. I. (2023) Novel Synthesis of CuO/GO Nanocomposites and Their Photocatalytic Potential in the Degradation of Hazardous Industrial Effluents. *ACS Omega*, **8**, 17667–17681.

27. Dien, N. D., Giang, T. D. T., Ha, P. T. T., Vu, X. H., Dung, N. T. and Trang, T. T. (2023) Developing efficient CuO nanoplate/ZnO nanoparticle hybrid photocatalysts for methylene blue degradation under visible light. *RSC Advances*, **13**, 24505.

28. Kumar, M., Mehta, A., Mishra, A., Singh, J., Rawat, M. and Basu, S. (2018) Biosynthesis of tin oxide nanoparticles using *Psidium guajava* leave extract for photocatalytic dye de- gradation under sunlight. *Materials Letters*, **215**, 121–124.

29. Anjum, M., Miandad, R., Waqas, M., Gehany, F. and Barakat, M. A. (2019) Remediation of wastewater using various nano-materials. *Arabian Journal of Chemistry*, **12**, 4897–4919.

30. Raghav, R., Aggarwal, P. and Srivastava, S. (2016) Tailoring oxides of copper-Cu_2O and CuO nanoparticles and evaluation of organic dyes degradation. In: *AIP Conference Proceedings*, **1724**, 020078.

31. Watt, B. E., Proudfoot, A. T. and Vale, J. A. (2004) Hydrogen peroxide poisoning. *Toxicological Reviews*, **23**, 51–57.

32. Matsumura, Y., Ananthaswamy, H, N. (2004) Toxic effects of ultraviolet radiation on the skin. *Toxicology and Applied Pharmacology*, **195**, 298–308.

33. Ejhieh and Banan, Z. (2012) Sunlight assisted photodecolorization of crystal violet catalyzed by CdS nanoparticles embedded on zeolite. *Desalination*, **284**, 157–166.

34. Ejhieh, A, N. and Shamsabadi, M. K. (2013) Decolorization of a binary azo dyes mixture using CuO incorporated nanozeolite-X as a heterogeneous catalyst and solar irradiation. *Biochemical Engineering Journal*, **228**, 631–641.

35. Pandey, S. and Mishra, S. B. (2014) Catalytic reduction of p-nitrophenol by using platinum Nanoparticles stabilised by guar gum. *Carbohydrate Polymers*, **113**, 525–531.

36. Mandlimath, T. R. and Gopal, B. (2011) Catalytic activity of first row transition metal oxides in the conversion of p-nitrophenol to p-anninophenol. *Journal of Molecular Catalysis A. Chemical*, **350**, 9–15.

37. El-Sheikh, S. M., Ismail, A. A., Al-Sharab, J. F. (2013) Catalytic reduction of p- nitrophenol over precious metals/highly ordered mesoporous silica. *New Journal of Chemistry*, **37**, 2399–2407.

38. Pradhan, N., Pal, A. and Pal, T. (2001) Catalytic Reduction of Aromatic Nitro Compounds by Coinage Metal Nanoparticles. *Langmuir*, **17**, 1800−1802.

39. Chhikara, N., Kaur, R., Jaglan, S., Sharma, P., Gata, Y. and Panghal, A. (2018) Bioactive compounds and pharmacological and food applications of *Syzygium cumini* – a review. *Food & Function*, **9**, 6096–6115.

40. Mehr, E. S., Sorbiun, M., Ramazani, A. and Fardood, S. T. (2018) Plant-mediated synthesis of zinc oxide and copper oxide nanoparticles by using Ferulagoangulata (Schlecht) Boiss extract and comparison of their photocatalytic degradation of Rhodamine B (RhB) under visible light irradiation. *Journal of Materials Science: Materials in Electronics*, **29**, 1333–1340.

41. Bala, N., Sarkar, M., Maiti, M., Nandy, P., Basud, R., Das, S. (2017) Phenolic compound-mediated single-step fabrication of copper oxide nanoparticles for elucidating their influence on anti-bacterial and catalytic activity. *New Journal of Chemistry*, **41**, 4458–4467.

42. Hammad, E. N., Salem, S. S., Zohair, M. M., Mohamed, A. A. and El-Dougdoug, W. (2022) *Purpureocillium lilacinum* mediated biosynthesis copper oxide nanoparticles with promising removal of dyes. *Biointerface Research in Applied Chemistry*, **12(2)**, 1397–1404.

43. Rafique, M., Tahir, M. B., Irshad, M., Nabi, G., Gillani, S. S. A., Iqbal, T. and Mubeen, M. (2020) Novel *Citrus aurantifolia* Leaves Based Biosynthesis of Copper Oxide Nanoparticles for Environmental and Wastewater Purification as an Efficient Photocatalyst and Antibacterial Agent. *Optik*, **219**, 165138.

44. Singh, J., Kumar, V., Kim, K. H. and Rawat, M. (2019) Biogenic synthesis of copper oxide nanoparticles using plant extract and its prodigious potential for photocatalytic degradation of dyes. *Environmental Research*, **177**, 108569.

45. Vasantharaj, S., Sathiyavimal, S., Saravanan, M., Senthilkumar, P., Kavitha, G., Shanmugavel, M., Manikandan, E. and Pugazhendhi, A. (2018) Synthesis of ecofriendly copper oxide nanoparticles for fabrication over textile fabrics: characterization of antibacterial activity and dye degradation potential. *Journal of Photochemistry and Photobiology B: Biology*, **191**, 149–155.

46. Maham, M., Sajadi, S. M., Kharimkhani, M. M. and Nasrollahzadeh, M. (2017) Biosynthesis of the CuO nanoparticles using *Euphorbia Chamaesyce* leaf extract and investigation of their catalytic activity for the reduction of 4-nitrophenol. *IET Nanobiotechnol*, **11**, 766–772.

47. Jafarirad, S., Rasoulpour, I., Divband, B., Hammami, I. and Kosari-nasab, M. (2018) Innovative biocapped CuO nano-photocatalysts: a rapid and green method for photocatalytic degradation of 4-nitrophenol. *Materials Research Innovation*, **22**, 415–421.

48. Bhattacharjee, A. and Ahmaruzzaman, M. (2018) Microwave assisted facile and green route for synthesis of CuO nanoleaves and their efficacy as a catalyst for reduction and degradation of hazardous organic compounds. *Journal of Photochemistry and Photobiology A*, **353**, 215–228.

49. Sankar, R., Manikandan, P., Malarvizhi, V., Fathima, T., Shivashangari, K. S. and Ravikumar, V. (2014) Green synthesis of colloidal copper oxide nanoparticles using Carica papaya and its application in photocatalytic dye degradation. *Spectrochimica Acta Part A: Molecular and Biomolecular Spectroscopy.* **121**, 746–50.

50. Vidovix, T. B., Quesada, H. B., Januario, E. F. D., Bergamasco, R., Vieira, A. M. S. (2019) Green synthesis of copper oxide nanoparticles using Punicagranatum leaf extract applied to the removal of methylene blue. *Materials Letters*, **257**, 126685.

51. Bordbar, M., Negahdar, N., Nasrollahzadeh, M. (2018) *Melissa Officinalis* L. leaf extract assisted green synthesis of CuO/ZnOnanocomposite for the reduction of 4-nitrophenol and Rhodamine B. *Separation and Purifcation Technology*, **191**, 295–300.

52. Rathi, B. S., Ewe, L. S., Sanjay, S., Sujatha, S., Yew, W. K., Baskaran, R. and Tiong, S. K. (2024) Recent trends and advancement in metal oxide nanoparticles for the degradation of dyes: synthesis, mechanism, types and its application. *Nanotoxicology*, **18(3)**, 272–298.

53. Bordbar, M., Sharifi-Zarchi, Z. and Khodadadi, B. (2017) Green synthesis of copper oxide nanoparticles/clinoptilolite using Rheum palmatum L. root extract: high catalytic activity for reduction of 4-nitro phenol, rhodamine B, and methylene blue. *Journal of Sol Gel Science Technology*, **81**, 724–733.

54. Sreeju, N., Rufus, A. and Philip, D. (2017) Studies on catalytic degradation of organic pollutants and anti-bacterial property using biosynthesized CuO nanostructures. *Journal of Molecular Liquids*, **242**, 690–700.

55. Zaman, M. A. and Bhattacharjee, A. (2016) CuO nanostructures: Facile synthesis and applications for enhanced photodegradation of organic compounds and reduction of p-nitrophenol from aqueous phase. *RSC Advances*, **6**, 41348–41363.

56. Qasem, M., Kurdi, R. E. and Patra, D. (2020) Green Synthesis of Curcumin Conjugated CuO Nanoparticles for Catalytic Reduction of Methylene Blue. *Chemistry Select*, **5**,1694 –1704.

57. Gu, H., Chen, X., Chen, F., Zhou, X. and Parsaee, Z. (2018) Ultrasound-assisted Biosynthesis of CuO NPs using Brown Alga *Cystoseiratrinodis*: Characterization, Photocatalytic AOP, DPPH Scavenging and Antibacterial Investigations. *Ultrasonics Sonochemistry*, **41**, 109–119.

58. Zhu, L., Li, H., Liu, Z., Xia, P., Xie, Y. and Xiong, D. (2018) Synthesis of 0D/3D CuO/ZnO Hetero junction with Enhanced Photocatalytic Activity. *Journal of Physical Chemistry C*, **122**, 9531–9539.

59. Nasrollahzadeh, M., Maham, M. and Sajadi, S. M. (2015) Green synthesis of CuO nanoparticles by aqueous extract of Gundeliatournefortii and evaluation of their catalytic activity for the synthesis of N-monosubstitutedureas and reduction of 4-nitrophenol. *Journal of Colloid and Interface Science*, **455**, 245–253.

60. Nazim, M., Khan, A. A. P. A., Asiri, M. and Kim, J. H. (2021) Exploring Rapid Photocatalytic Degradation of Organic Pollutants with Porous CuO Nanosheets: Synthesis, Dye Removal, and Kinetic Studies at Room Temperature. *ACS Omega*, **6(4)**, 2601–2612.

61. Bordbar, M., Sharifi-Zarchi, Z. and Khodadadi, B. (2017) Green synthesis of copper oxide nanoparticles/clinoptilolite using *Rheum palmatum L* root extract: high catalytic activity for reduction of 4-nitro phenol, rhodamine B, and methylene blue. *Journal of Sol-Gel Science and Technology*, **81**, 724–733.

62. Sharma, A., Dutta, R. K., Roychowdhury, A., Das, D., Goyal, A. and Kapoor, A. (2018) Cobalt doped CuO nanoparticles as a highly efficient heterogeneous catalyst for reduction of 4-

nitrophenol to 4-aminophenol. *Applied Catalysis A. General*, **543**, 257–265.

63. Sreeju, N., Rufus, A and Philip, D. (2017) Studies on catalytic degradation of organic pollutants and anti-bacterial property using biosynthesized CuO nanostructures. *Journal of Molecular Liquids*, **242**, 690–700.
64. Zaman, M. A. and Bhattacharjee, A. (2016) CuO nanostructures: Facile synthesis and applications for enhanced photodegradation of organic compounds and reduction of p-nitrophenol from aqueous phase. *RSC Advances*, **6**, 41348–41363.
65. Bouazizi, N., Vieillard, J., Thebault, P., Desirac, F., Clamens, T., Bargougui, R., Couvrat, N., Thoumire, O., Brun, N., Ladam, G., Morin, S., Mofaddel, N., Lesouhaitier, O., Azzouz, A. and Le Derf, F. (2018) Silver Nanoparticles Embedded Copper Oxide as Efficient Core- Shell for Catalytic Reduction of 4-nitrophenol and Antibacterial Activity improvements. *Dalton Transactions*, **47**, 9143–9155.
66. Baloch, G. N. L., Mahesar, S. A., Khan, S., Niisa, J. and Sherazi, R. S. T. H. (2020) Ranolazine-functionalized CuO NPs: efficient homogeneous and heterogeneous catalysts for reduction of 4-nitrophenol. *Turkish Journal of Chemistry*, **44**, 168–179.